Analysis and modelling of process conditions influencing N_2O emission by aerobic granular sludge processes for N/DN treatment

Mathieu POCQUET[1, 2, 3, 4, 5], Ahlem FILALI[1, 2, 3], Yolaine BESSIERE[1, 2, 3], Lisha GUO[4], Isabelle QUEINNEC[5], Peter A. VANROLLEGHEM[4], Mathieu SPERANDIO*[1, 2, 3]

[1] Université de Toulouse; INSA, UPS, INP; LISBP, 135 Avenue de Rangueil, F-31077 Toulouse, France
[2] INRA, UMR792 Ingénierie des Systèmes Biologiques et des Procédés, F-31400 Toulouse, France
[3] CNRS, UMR5504, F-31400 Toulouse, France
[4] model*EAU*, Université Laval, Département de génie civil et de génie des eaux, 1065 av. de la Médecine, Québec (QC), G1V 0A6, Canada.
[5] CNRS ; LAAS ; 7 avenue du colonel Roche, F-31077 Toulouse Cedex 4, France

Abstract
Nitrous oxide (N_2O) can be emitted by an aerobic granular sludge process during nitrification and denitrification. In this work lab-scale sequencing batch airlift reactors (SBR) were run in varying conditions in order to identify a mathematical model. The increase of the N_2O production rate in the case of nitrite accumulation was quantified and simulated. The assumption of a direct correlation (instead of reverse AOB nitrite reduction) turned out to be more efficient to predict the observations. A biofilm model including granules based on a modified ASM3 model including N_2O and NO production was finally proposed and adjusted to experimental data.

Keywords
denitrification; granular sludge process; greenhouse gases; modelling; nitrification; nitrous oxide.

INTRODUCTION

The aerobic granular sludge process is considered as one of the most promising processes in wastewater treatment (De Kreuk et al., 2009; Wan et al., 2009). However, nitrous oxide (N_2O), a greenhouse gas, can be emitted during this process as in most biological nitrification / denitrification processes (Kampschreur et al., 2009). It is therefore of great importance to investigate the conditions which minimize this production and to propose optimal operating strategies. Modelling may then represent a very useful tool in view of a better understanding of N_2O emissions. During nitrification with conventional activated sludge, it was demonstrated that N_2O emission is increased at low DO concentration and also at high nitrite concentration (Kampschreur et al., 2009). Denitrification is also reported to particularly produce N_2O at low COD/N ratios (Hiatt and Grady, 2008). In this study, a granular sludge sequencing batch reactor is considered, where nitrification and denitrification generally occur simultaneously thanks to the presence of aerobic and anoxic zones within the granule. Experiments were then performed in order to evaluate the respective N_2O production via nitrification and denitrification and the specific effect of nitrite accumulation. Nitrification models from literature are compared to experimental data. A general biofilm model is then proposed based on a modified version of ASM3 including the four steps denitrification of the ASMN model (Hiatt and Grady, 2008). This modified model also includes a N_2O production model chosen among three potential models of N_2O production.

MATERIALS AND METHODS

Experimental set-up

The Granular Sequencing Batch Reactor (GSBR) with a working volume of 17 L (internal diameter = 15 cm, total height =105 cm, H/D ratio = 7) was operated with a biomass concentration of 17.9

gTSS.L^{-1} (90% of granules, 10% of flocs). Each 4 hour cycle of the GSBR was operated in five successive steps: a first non-aerated feeding step (15 min), an anoxic step (20 min), an aerobic step (145 min), a settling step (30 min) and a discharge step of 30 minutes (with a volumetric exchange ratio of 47%). Nitrogen gas (anoxic step) and air (aerobic step) was sparged at 350 L h^{-1}. The GSBR has been fed during two years with a synthetic substrate composed of: COD with a concentration of 1000 mg L^{-1} (25% contribution each of glucose, acetate, propionic acid and ethanol), [PO_4^{3-}] = 30 mgP L^{-1} , [Ca^{2+}] = 46 mg L^{-1}, [HCO_3^-] = 100 mg L^{-1}, [$MgSO_4 \cdot 7H_2O$] = 12 mg L^{-1}, [NH_4^+] = 50 mgN L^{-1}, [NO_3^-] = 100 mgN L^{-1}. pH, temperature and oxygen were measured (WTW probes) and monitored every 30 seconds. The temperature has been maintained at 20 ± 2 °C with a water jacket. Nitrous oxide has been measured into the gas phase on the top of the GSBR by an X-STREAM X2GP gas analyzer (Infra-Red channel; Sample flow: 0.2 L min^{-1}; Range: 0-100 ppm). Chemical analyses were obtained with ionic chromatography (IC25, 2003, DIONEX, USA), in which NO_2^-, NO_3^-, PO_4^{3-}, NH_4^+, Ca^{2+}, K^+, Mg^{2+} concentrations were determined with prior filtering of the samples through a 0.2 µm pore-size acetate filter. Suspended solids concentration was determined according to Standards methods (AFNOR 1994).

Model description

A model based on ASM3 and ASMN has been developed to describe the biological nitrogen removal by nitrification/denitrification and the N_2O production associated with these processes. To describe AOB and NOB growth and N_2O production by AOB, three models have been compared. Figure 1 presents the schematic representations of the scenario A of the model of Mampaey et al. (2011), the model of Ni et al. (2011) and the model of Houweling et al. (2011).

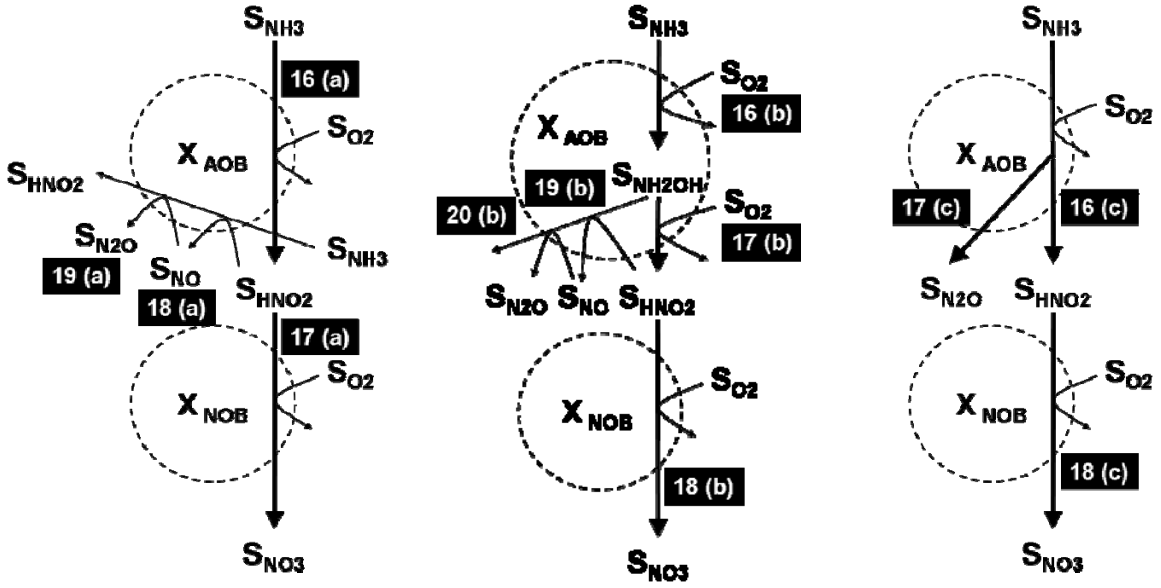

(a) (b) (c)

Figure 1. (a) Scenario A of the model of Mampaey et al. (2011). (b) Model of Ni et al. (2011). (c) Model of Houweling et al. (2011). Numbers refer to the Gujer matrix of Table 1.

Models (a) and (b) are based on the nitrifier denitrification process. Model (c) considers that a fraction of ammonia is directly converted into N_2O. In this last model, the fraction of ammonia converted to N_2O is proportional to the nitrite concentration via a correlation function as proposed by Houweling *et al.* (2011). Aerobic and anoxic endogenous respiration of AOB and NOB have also been considered using O_2, NO_3^- and NO_2^- as electron acceptor (even if these last processes

consume negligible amounts of electron acceptors) considering that organic matter released by bacteria lysis is logically used by heterotrophic bacteria as electron donor. True substrate concentrations of free ammonia (FA: N-NH_3) and free nitrous acid (FNA: N-HNO_2) (of AOB and NOB respectively) are calculated according to the formulation of Hiatt and Grady (corrected by Corominas et al., 2012, for the form FNA). To calculate these N forms, temperature and pH of the GSBR cycles have been included in the model.

In the original model ASM3, the heterotrophic growth processes include a first step of storage of soluble substrate into storage compounds. These storage compounds are used as carbon source for the aerobic and anoxic growth of heterotrophic biomass. As proposed by Sin et al. (2005) simultaneous storage and growth on easily biodegradable substrate has also been included. The second modification of the original ASM3 model consists of differentiating between ammonium oxidizing bacteria (AOB) and nitrite oxidizing bacteria (NOB). Then additional mechanisms have been introduced for description of nitric oxide and nitrous oxide production. Concerning anoxic growth of heterotrophic biomass, the basis of the ASMN model proposed by Hiatt and Grady (2008) has been used. All processes associated to the heterotrophic biomass are presented in figure 1. Hydrolysis of particulate biodegradable organics has not been considered since only soluble biodegradable organics are present in the synthetic substrate.

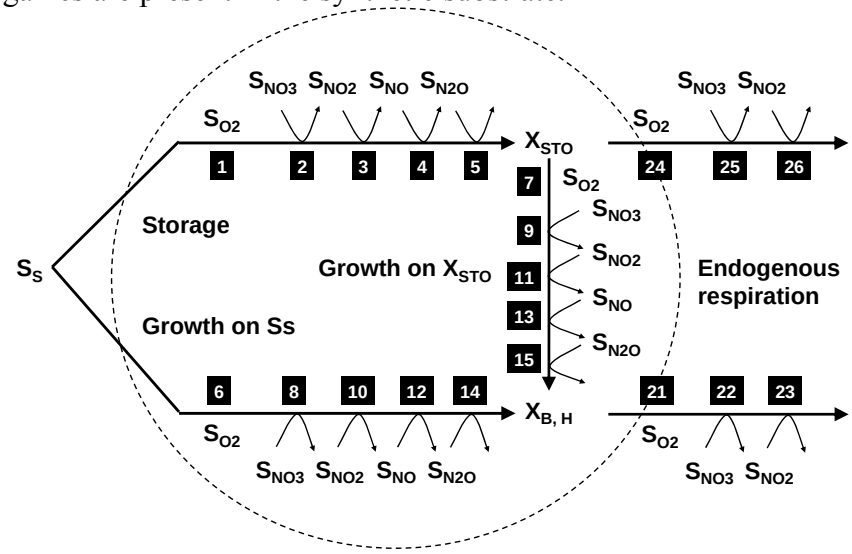

Figure 2. Schematic representation of heterotrophic processes in aerobic and anoxic conditions.

Figure 2 illustrates the different flows of the organic carbon which can be used (by growth, storage, endogenous respiration) either in aerobic or anoxic conditions. During the anoxic phase, these processes have been all divided into four steps: nitrate, nitrite, nitric oxide and nitrous oxide are successively used as electron acceptor. Aerobic and anoxic endogenous respiration of storage compounds and heterotrophic biomass of ASM3 has also been included using nitrite and nitrate as electron acceptors.

AQUASIM software version 2.1g (Reichert, 1998) has been used to implement the biofilm model. Granules are considered as spherical particles with a constant diameter (3 mm, measured experimentally). Each granule is divided into 10 layers which allow describing a biomass concentration distribution and species gradients. The total number of granules was estimated considering the VSS concentration, volumetric fraction of solids in the reactor, and the granules density. Overall, the model is composed of 21 processes for heterotrophic biomass (including storage processes), 11 processes for the physical and operational processes (including NO and N_2O stripping during anoxic and aerobic phase, air inflow and sludge removal), 6 processes for

autotrophic biomass (including endogenous respiration similar to heterotrophic organisms) in addition to 4 processes for model (a); 5 for model (b) or 3 for model (c).

RESULTS AND DISCUSSION

Analysis of experimental data

The data obtained indicate that the N_2O production rate depends a lot on the conditions maintained in the reactor cycle, and ranged from less than 1% of the removed nitrogen to more than 15 % (in the worst conditions). The N_2O production rate during nitrification increases with nitrite accumulation. It varies from 0.1 to 8% of the nitrified nitrogen when nitrite was artificially dosed from 0 to 20 mgN/L (figure 5). When nitrogen was eliminated by SND via the nitrite route (the absence of NOB was demonstrated by FISH measurements by Filali et al., 2012) with a DO in the bulk of 4-6 mg/L the N_2O production rate was stabilized at less than 1.4% of the removed nitrogen, which is comparable to the range of values reported in activated sludge processes. Comparison with data collected with GSBR suggest that simultaneous denitrification of nitrite within the granules reduces the N_2O production rate.

Nitrification modelling

Only autotrophic processes were considered in a first modelling phase which only considers the activated sludge part (no granules considered) to simplify the analysis. The different nitrification models (a), (b) and (c) were evaluated comparing simulations to the profile obtained during the aerobic phase of the GSBR. Indeed during this period the reactor was operated with a negligible SND (mainly due to high DO) as demonstrated by conservation of total nitrogen. The Gujer matrix of the autotrophic processes is given in table 1 for each model.

The maximal growth rates of AOB and NOB species were first slightly adjusted in order to accurately predict the ammonia, nitrite and nitrate forms. A similar initial biomass concentration of AOB and NOB was assumed for all models, respectively 37.0 $gDCO.m^{-3}$ and 26.4 $gDCO.m^{-3}$ determined by parameter estimation using default values of Houweling et al. (2011). Simulation results are presented in figure 3 and figure 4. All models have a similar capacity to predict ammonia, nitrite and nitrate concentrations during standard aerobic cycle (figure 3) as well as a cycle with extra nitrite (figure 4).

As shown by figure 3, the measured nitrous oxide production rate is low at the beginning of the aerobic phase. It progressively increases up to a maximum value when the nitrite concentration reaches a maximal value, corresponding to the time when ammonia is depleted. Indeed, the nitrous oxide concentration in the gas phase increase to 4 ppm in 80 minutes. Then the ammonia concentration tends to zero and the nitrite concentration decreases as well as the nitrous oxide concentration in the gas phase. Models (a) and (b) were not able to predict this tendency even after a significant parameter adjustment. Moreover, both of them underestimated the amount of N_2O produced. For a normal aerobic cycle, model (a) predicts a maximum production of 0.5 ppm of nitrous oxide and 37.4 ppm of nitric oxide. Model (b) predicts a maximum production of 0.008 ppm of nitrous oxide and 0.66 ppm of nitric oxide. In these models, the production rate of nitrous oxide is too weak compared to the aeration rate and nitric oxide is stripped before being transformed into nitrous oxide.

Table 1. Gujer matrix of nitrification models (a) (b) and (c).

		S_{N2O}	S_{NO}	S_{NH}	S_{NH2OH}	S_{NO2}	S_{NO3}	S_O	X_{AOB}	X_{NOB}
Mampaey	16(a)			-inbm-1/Y_{AOB}		1/Y_{AOB}		-(3.43-Y_{AOB})/Y_{AOB}	1	
	17(a)			-inbm		-1/Y_{NOB}	1/Y_{NOB}	-(1.14-Y_{NOB})/Y_{NOB}		1
	18(a)		2/Y_{AOB}	-inbm-1/Y_{AOB}		-1/Y_{AOB}		-(2.29-Y_{AOB})/Y_{AOB}	1	
	19(a)	2/Y_{AOB}	-2/Y_{AOB}	-inbm-1/Y_{AOB}		1/Y_{AOB}		-(2.29-Y_{AOB})/Y_{AOB}	1	
	16(a)	$\mu_{AOB}*S_O/(S_O+K_{O,AOB})*S_{FA}/(S_{FA}+K_{FA})*X_{AOB}$								
	17(a)	$\mu_{NOB}*S_O/(S_O+K_{O,NOB})*S_{FNA}/(S_{FNA}+K_{FNA,NOB})*K_{I,FA,NOB}/(K_{I,FA,NOB}+S_{FA})*X_{NOB}$								
	18(a)	$\eta_{AOB}*\mu_{AOB}*S_O/(S_O+K_{O,AOB})*S_{FA}/(S_{FA}+K_{FA})*S_{NO2}/(S_{NO2}+K_{NO2,AOB})*X_{AOB}$								
	19(a)	$\eta_{AOB}*\mu_{AOB}*S_O/(S_O+K_{O,AOB})*S_{FA}/(S_{FA}+K_{FA})*S_{NO}/(S_{NO}+K_{NO,AOB})*X_{AOB}$								
Ni	16(b)			-1	1			-1.14		
	17(b)				-1/Y_{AOB}	1/Y_{AOB}		-(2.29-Y_{AOB})/Y_{AOB}	1	
	18(b)			-inbm		-1/Y_{NOB}	1/Y_{NOB}	-(1.14-Y_{NOB})/Y_{NOB}		1
	19(b)		4		-1	-3				
	20(b)	4	-4		-1	1				
	16(b)	$\mu_{AOB,AMO}*S_O/(S_O+K_{O,AOB,S1})*S_{FA}/(S_{FA}+K_{FA\_AOB})*X_{AOB}$								
	17(b)	$\mu_{AOB,HAO}*S_O/(S_O+K_{O,AOB,S2})*S_{NH2OH}/(S_{NH2O}H+K_{NH2OH,AOB})*X_{AOB}$								
	18(b)	$\mu_{NOB}*S_O/(S_O+K_{O,NOB})*S_{FNA}/(S_{FNA}+K_{FNA,NOB})*K_{I,FA,NOB}/(K_{I,FA,NOB}+S_{FA})*X_{NOB}$								
	19(b)	$\eta_{AOB}*\mu_{AOB,HAO}*K_{I,O,AOB}/(S_O+K_{I,O,AOB})*S_{NO2}/(S_{NO2}+K_{NO2,AOB})*S_{NH2OH}/(S_{NH2OH}+K_{NH2OH,AOB})*X_{AOB}$								
	20(b)	$\eta_{AOB}*\mu_{AOB,HAO}*K_{I,O,AOB}/(S_O+K_{I,O,AOB})*S_{NO}/(S_{NO}+K_{NO,AOB})*S_{NH2OH}/(S_{NH2OH}+K_{NH2OH,AOB})*X_{AOB}$								
Houweling	16(c)			-1/Y_{AOB}-inbm		1/Y_{AOB}		-(3.43-Y_{AOB})/Y_{AOB}	1	
	17(c)	1/Y_{AOB}		-1/Y_{AOB}				-2.29/Y_{AOB}		
	18(c)			-inbm		-1/Y_{NOB}	1/Y_{NOB}	-(1.14-Y_{NOB})/Y_{NOB}		1
	16(c)	$\mu_{AOB}*S_O/(S_O+K_{O,AOB})*S_{FA}/(S_{FA}+K_{FA\_AOB})*X_{AOB}*((1+\exp(Slope*(S_{NO2}/(S_{NO2}+K_{NO2})-K)))^{(-1)})$								
	17(c)	$\mu_{AOB}*S_O/(S_O+K_{O,AOB})*S_{FA}/(S_{FA}+K_{FA\_AOB})*X_{AOB}*(1-((1+\exp(Slope*(S_{NO2}/(S_{NO2}+K_{NO2})-K)))^{(-1)}))$								
	18(c)	$\mu_{NOB}*S_O/(S_O+K_{O,NOB})*S_{FNA}/(S_{FNA}+K_{FNA,NOB})*K_{I,FA,NOB}/(K_{I,FA,NOB}+S_{FA})*X_{NOB}$								

These models underestimated the effect of additional nitrite on the N_2O production rate. As shown by figure 4, an injection of 10 mgN-NO_2 L^{-1} leads to a larger nitrous oxide production. The maximum gas phase concentration observed is 13.9 ppm at 77 min. In these conditions, model (a) and (b) are not able to predict this production dynamics with a maximum concentration of 0.68 ppm of N_2O and 52.1 ppm of NO for model (a) and 0.008 ppm of N_2O and 0.66 ppm of NO for model (b). On the other hand model (c) is able to predict a nitrous oxide concentration in the same order of magnitude as the experimental data for each cycle in figure 3 and 4. However, the correlation function of the Houweling model has to be adapted for an accurate prediction. Here the best K_{NO2} value (of CF factor) is 13.3, 18.2 and 29.6 mgN-NO_2.L^{-1} for initial nitrite additions of 0, 10 and 20 mgN-NO_2.L^{-1} respectively. Thus it means that this model can catch qualitatively the N_2O production dynamics when nitrite accumulates, but still needs adaptation to predict the quantity of N_2O produced for a large range of nitrite concentrations. This seems logical as the CF expression has been chosen arbitrarily by Houweling et al. (2011) but does not correspond to any real physical or biochemical process. This fitted expression is thus only valuable over a limited range of nitrite concentrations.

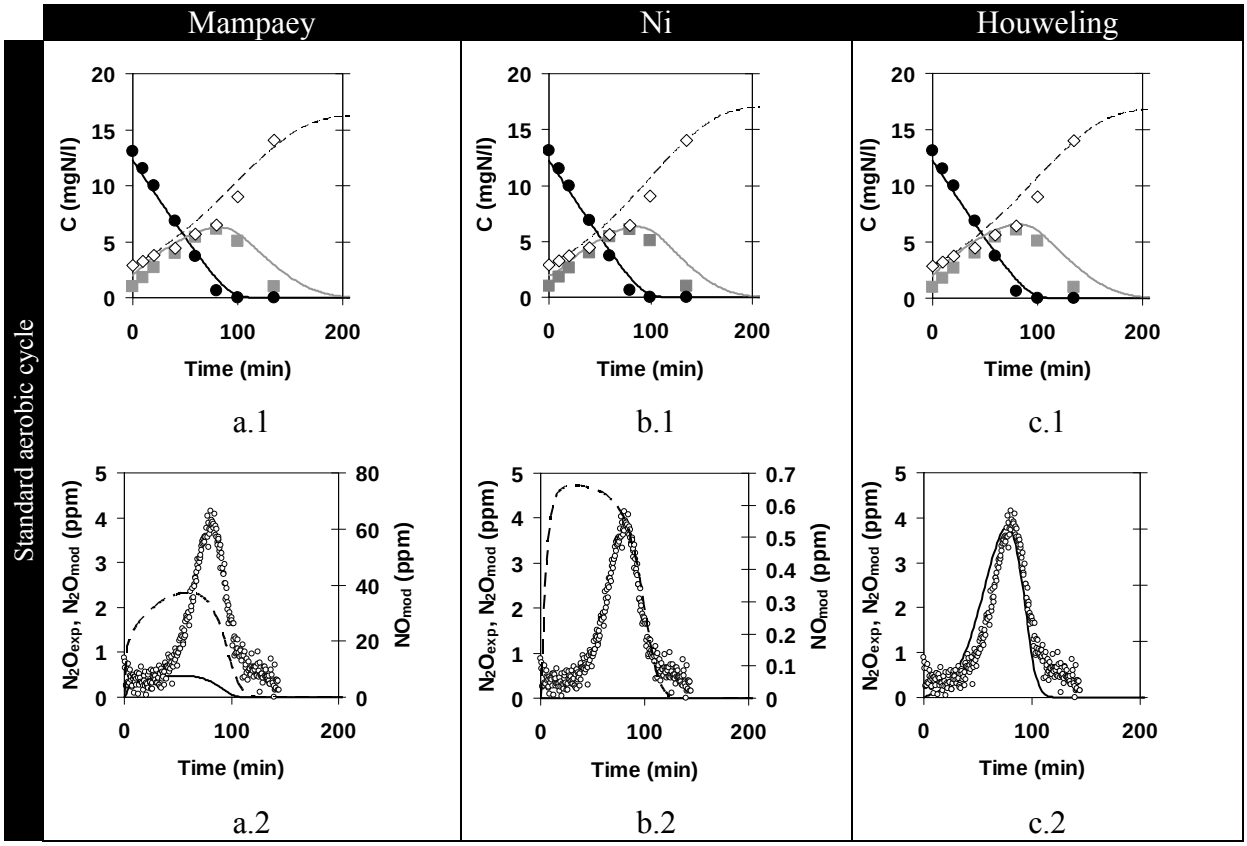

Figure 3. Nitrification model analysis for a normal aerobic cycle. In line 1, experimental data are represented by markers ((●) Total ammonia concentration; (■) Nitrite concentration; (◊) Nitrate concentration) whereas lines correspond to simulation results. In line 2: (○) experimental N_2O in gas; (---) modeled Nitric oxide ; (-) modeled N_2O. Column "a" Mampaey's model, column "b" Ni's model and column "c": Houweling's model.

Results with global modified ASM3 model

Model (c) has been included in the modified ASM3 model (with a fitted set of parameter for the correlation function, see Appendix). For each scenario, a preliminary long term simulation has been used to obtain the biomass distribution in the granule layers (steady state reached after two hundred days of simulation). In figure 5, the anoxic and aerobic phases of each cycle are presented and simulations with the global model are compared to the data.

Denitrification occurs during the first 20 minutes of the GSBR cycle. Soluble COD is converted by heterotrophic organisms into carbon dioxide (growth) or into storage compounds. The production of N_2O during anoxic phase predicted by the model is of the same order of magnitude as the experimental data. In these processes, nitrite, nitrate, nitric oxide and nitrous oxide are used as electron acceptor and reduced into the N-form with the lower oxidation state. Nitrate and nitrite reduction simulations correspond to the experimental characterization and tend to zero at the end of the anoxic phase (at 20 minutes, there is 1.1 and 0.8 mgN-NO_2^- L^{-1} and 3.3 and 1.8 mg N-NO_3^- L^{-1} in the soluble phase for the cycle without perturbations and the cycle "10 mgN-NO_2^- L^{-1}" respectively). The COD/N ratio of 10 allows a total consumption of COD and nitrogen forms in the soluble phase during this first anoxic step and determines the efficiency of the next aerobic phase. About 0.06 to 0.1 % of the denitrified nitrate is converted to N_2O during the anoxic phase.

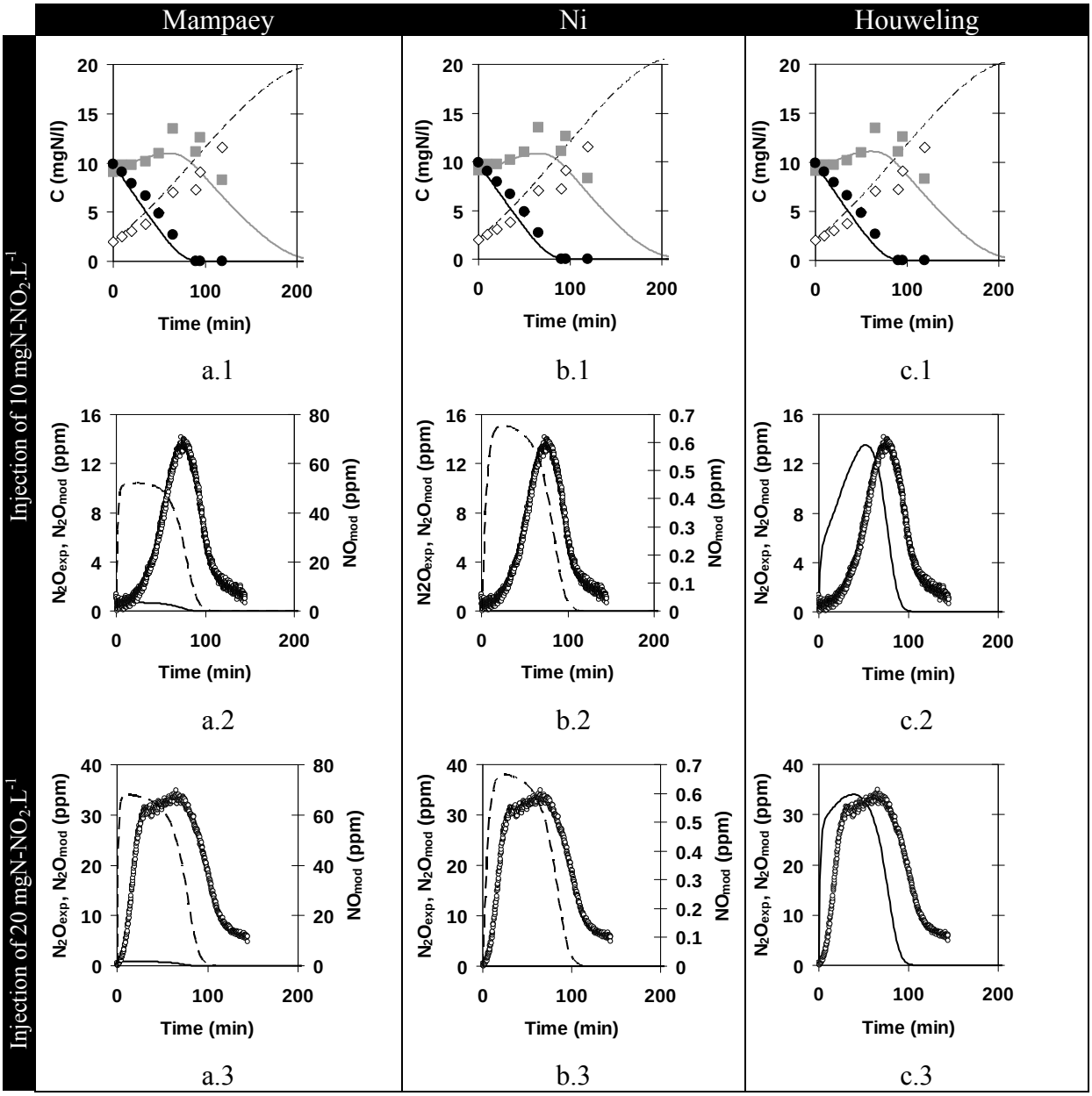

Figure 4. Nitrification responses following nitrite injection. Lines 1 and 2 correspond to an injection of 10 mgN-NO_2^- L^{-1} and line 3 corresponds to an injection of 20 mgN-NO_2^- L^{-1} at the beginning of the cycle. In line 1, experimental data are represented by markers ((●) Total ammonia concentration; (■) Nitrite concentration; (◊) Nitrate concentration) whereas lines correspond to simulation results. In lines 2 and 3: (○) experimental N_2O in gas; (---) modeled Nitric oxide; (-) modeled N_2O. Column "a" Mampaey's model, column "b" Ni's model and column "c": Houweling's model.

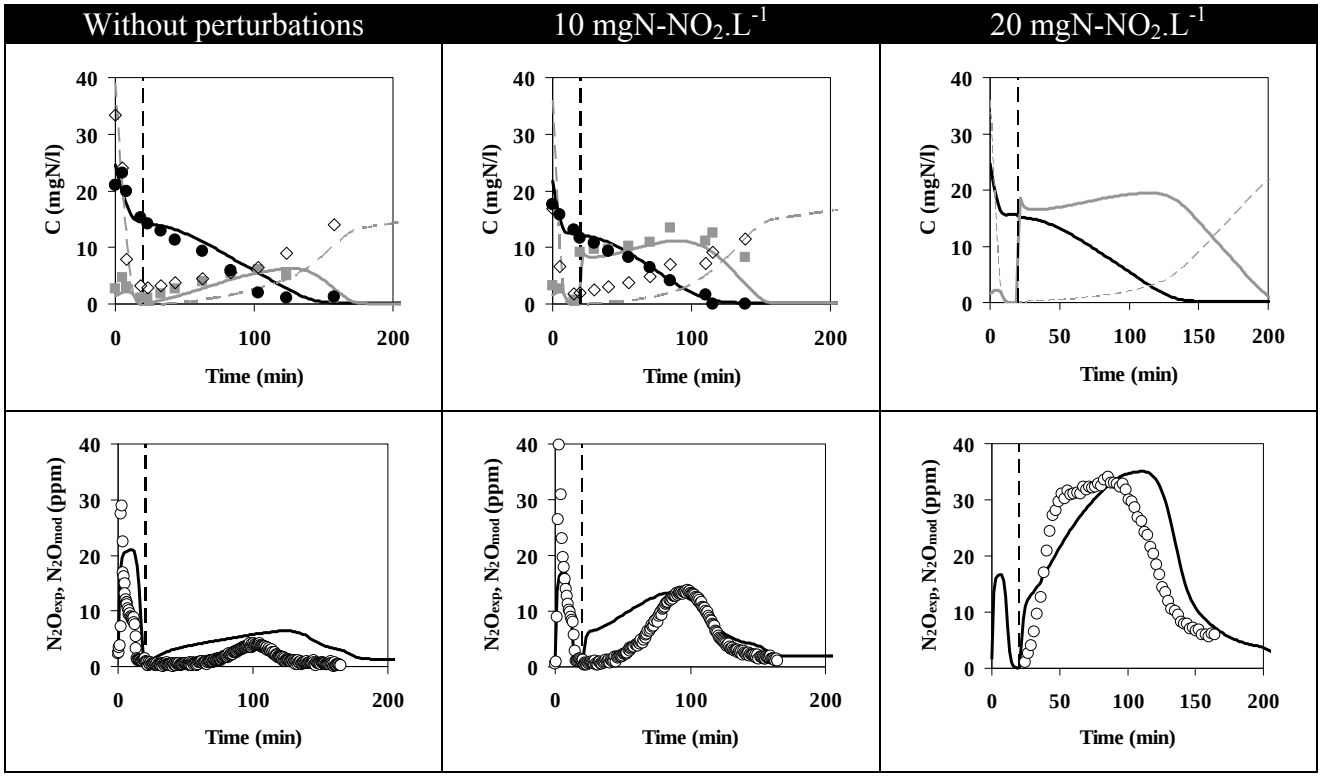

Figure 5. ASM3 modified plus model (c). (●) Total ammonia concentration; (■) Nitrite concentration; (◊) Nitrate concentration; (○) experimental N_2O in gas; (-) modeled N_2O. Vertical dashed line differentiates the 20 minutes anoxic phase from the 120 minutes aerobic phase.

During the aerobic phase without NO_2^- addition, the nitritation rate is slightly underestimated whereas this dynamics is predicted accurately after 10 mgN-NO_2^- L^{-1} addition. AOB converts 14.2 mg N-NH_4.L^{-1} and 11.7 mg N-NH_4.L^{-1} in 103 and 90 minutes with 0 and 10 mgN-NO_2^- L^{-1} addition respectively. For the latter, the model overestimates the activity of NOB when ammonia tends to zero. That induces a good prediction of nitrite accumulation in the absence of NO_2^- addition and at the beginning of the aerobic phase when NO_2 was added. Nitrous oxide produced during aerobic phase is mainly due to nitrification but denitrification also contributes inside the granules. It is the reason why N_2O production is slightly overestimated in the initial period of the aerobic phase. Results were even worse when NO and N_2O production were also included in the endogenous processes (not shown). Hence, they were only included in the denitrification on readily biodegradable compounds and storage compounds. Table 2 shows the experimental and simulated total nitrous oxide production in the anoxic and aerobic phases of the GSBR.

Table 2. Total nitrous oxide production.

NO_2 addition (mg N-NO_2^-.L^{-1})	Phase	N_2O (mg N-N_2O.L^{-1}) Experimental	Simulated
0	Anoxic	0.06	0.13
	Aerobic	0.08	0.26
10	Anoxic	0.10	0.07
	Aerobic	0.31	0.48
20	Anoxic	*ND*	0.05

Aerobic	1.18	1.37

The data presented in table 2 show the capacity of the model to predict the order of magnitude of total nitrous oxide produced in both anoxic and aerobic phases. The N_2O concentration in the anoxic phase after addition of 20 mgN-NO_2^- L^{-1} were disturbed by previous cycles and the experimental data were not representative of a standard anoxic phase as in the other anoxic data sets. These results reveal the link between nitrite accumulation and nitrous oxide production during nitrification: if more nitrite is present in the soluble phase more nitrous oxide is produced by AOB during the aerobic phase.

CONCLUSION

The influence of nitrite accumulation on nitrous oxide production has been experimentally characterized and shows the importance of an accurate control of the nitrite level via SND in the granular sludge process. This link between nitrite and nitrous oxide can be described by a simplified model assuming that ammonia conversion into nitrite and nitrous oxide depends on the nitrite concentration in the soluble phase. However this correlation is not satisfying as it is not based on a biochemical mechanism and work is on its way to get a better mechanistic description of these transient N_2O emissions. The proposed modified ASM3 model allows an acceptable prediction capacity of the order of magnitude of nitrous oxide production during both anoxic and aerobic phases.

ACKNOWLEDGEMENT

The work of Mathieu Pocquet is funded by the French National Research Agency (project CreativERU). The authors would like to thank E. Mengelle, M. Bounouba, D. Delagnes and model*EAU* members for their help in this work. Peter Vanrolleghem holds the Canada Research Chair on Water Quality Modelling. Lisha Guo acknowledges the financial support obtained through the TECC project of the Québec Ministry of Economic Development, Innovation and Exports (MDEIE) and the research project funded by the Flemish Fund for Scientific Research (FWO - G.A051.10).

REFERENCES

Corominas, L.; Flores-Alsina, X.; Snip, L.; Vanrolleghem, P.A. (2012) Comparison of different modelling approaches to better understand and minimize greenhouse gas emissions from wastewater treatment plants. Biotechnol. Bioeng. DOI: 10.1002/bit.24544

Filali, A. (2011) Analyse et modélisation du traitement de l'azote dans un procédé de granulation aérobie hybride. PhD. thesis. Science des procédés, Institut National des Sciences Appliquées de Toulouse, France (in French).

Filali, A.; Mañas, A.; Mercade, M.; Bessière, Y.; Biscans, B.; Spérandio, M. (2012) Stability and performance of two GSBR operated in alterning anoxic/aerobic or anaerobic/aerobic conditions for nutrient removal. Biochem. Eng., 67, 10-19.

Henze, M.; Gujer, W.; Matsuo, T.; van Loosdrecht, M.C.M. (2000) Activated sludge models ASM1, ASM2, ASM2d and ASM3, Scientific and Technical Reports. IWA Publishing: London, UK.

Hiatt, W.C.; Grady, C.P.L.Jr. (2008) An updated process model for carbon oxidation, nitrification and denitrification, Water Environ. Res., 80, 2145-2156.

Houweling, D.; Wunderlin, P.; Dold, P.; Bye, C.; Joss, A.; Siegrist, H. (2011) N_2O emissions: Modeling the effect of process configuration and diurnal loading patterns. Water Environ. Res., 83, 2131-2139.

Kampschreur, M.J.; Temmink, H.; Kleerebezem, R.; Jetten, M.S.M.; van Loosdrecht, M.C.M. (2009) Nitrous oxide emission during wastewater treatment. Water Res., 43, 4093-4103.

Mampaey, K.E.; Beuckels, B.; Kampschreur, M.J.; Kleerebezem, R.; van Loosdrecht, M.C.M.; Volcke, E.I.P. (2011) Modelling nitrous and nitric oxide emissions by autotrophic ammonium oxidizing bacteria. In: Proceedings IWA/WEF Nutrient Recovery and Management 2011 Conference. Miami, FL (USA), 9-12 January 2011.

Ni, B.-J.; Ruscalleda, M.; Pellicer-Nacher, C.; Smets, B.F. (2011) Modeling nitrous oxide production during biological nitrogen removal via nitrification and denitrification: Extensions to the general ASM models. Environ. Sci. Technol., 45, 7768-7776.

Ni, B.-J.; Yuan, Z.; Chandran, K.; Vanrolleghem, P.A.; Murthy, S. (2012) Evaluating mathematical models for N_2O production by ammonia-oxidizing bacteria: Towards a unified model. In: Proceedings 3rd IWA/WEF Wastewater Treatment Modelling Seminar (WWTmod2012). Mont-Sainte-Anne, Québec, Canada, 26-28 February 2012.

NIST online database n°69. </http://webbook.nist.gov/chemistry/> (consulted on June 2012).

Reichert, P. (1998) AQUASIM 2.0—user manual, computer program for the identification and simulation of aquatic systems. Swiss Federal Institute for Environmental Science and Technology (EAWAG), Dubendorf, Switzerland.

Sin, G.; Guisasola, A.; De Pauw, D.J.W.; Baeza, J.A.; Carrera, J.; Vanrolleghem, P.A. (2005) A new approach for modelling simultaneous storage and growth processes for activated sludge systems under aerobic conditions. Biotechnol. Bioeng., 92, 600-613.

von Schulthess, R.; Gujer, W. (1996) Release of nitrous oxide (N_2O) from denitrifying activated sludge: Verification and application of a mathematical model. Water Res., 30, 521-530.

Wan, J.F.; Bessiere, Y.; Sperandio, M. (2009) Alternating anoxic feast/aerobic famine condition for improving granular sludge formation in sequencing batch airlift reactor at reduced aeration rate. Water Res., 43, 5097-5108.

APPENDIX

Table 3. Parameter values of the model. Source: (1) ASM3, (2) ASMN, (3) Filali (2011), (4) von Schulthess & Gujer (1996), (5) Ni et al. (2011), (6) NIST online database, (7) Houweling et al. (2011), (8) Fitted.

Symbol	Definition	Value	Unit	Source
b_{AOB}	Endogenous respiration rate for AOB - Aerobic	0.15	d^{-1}	(1)
$b_{AOB,anox}$	Endogenous respiration rate for AOB - Anoxic	0.0275	d^{-1}	(3)
b_{H}	Endogenous respiration rate for heterotrophic - Aerobic	0.2	d^{-1}	(1)
$b_{H,anox}$	Endogenous respiration rate for heterotrophic - Anoxic	0.055	d^{-1}	(3)
b_{NOB}	Endogenous respiration rate for NOB - Aerobic	0.15	d^{-1}	(1)
$b_{NOB,anox}$	Endogenous respiration rate for NOB - Anoxic	0.0275	d^{-1}	(3)
b_{STO}	Endogenous respiration rate for heterotrophic - Aerobic	0.2	d^{-1}	(1)
$b_{STO,anox}$	Endogenous respiration rate for heterotrophic - Anoxic	0.055	d^{-1}	(3)
K	Houweling correlation function parameter	0.9	$gN.m^{-3}$	(8)
Slope	Houweling correlation function parameter	10	-	(8)
K_{NO2}	Houweling correlation function parameter	8	-	(8)
D_{N2}	Diffusivity of N_2 in water	0.00017366	$m^2.d^{-1}$	(3)
D_{NH4}	Diffusivity of NH_4^+ in water	0.000141	$m^2.d^{-1}$	(3)
D_{NO2}	Diffusivity of NO_2^- in water	0.000137	$m^2.d^{-1}$	(3)
D_{NO3}	Diffusivity of NO_3^- in water	0.000137	$m^2.d^{-1}$	(3)
D_{O2}	Diffusivity of O_2 in water	0.00018	$m^2.d^{-1}$	(3)
D_S	Diffusivity of organic substrate in water	0.000104	$m^2.d^{-1}$	(3)
D_{N2O}	Diffusivity of N_2O in water	0.000177	$m^2.d^{-1}$	(4)
D_{NO}	Diffusivity of NO in water	0.000245	$m^2.d^{-1}$	(4)
ηg2	Anoxic growth reduction factor $NO_3^- \rightarrow NO_2^-$	0.28	-	(2)
ηg3	Anoxic growth reduction factor $NO_2^- \rightarrow NO$	0.16	-	(2)
ηg4	Anoxic growth reduction factor $NO \rightarrow N_2O$	0.35	-	(2)
ηg5	Anoxic growth reduction factor $N_2O \rightarrow N_2$	0.6	-	(2)
$ηg_{AOB}$	Anoxic reduction factor - Autotrophic organisms	0.074	-	(5)
fxi	Fraction of inert biomasse	0.2	-	(1)
inbm	N fraction of active biomass	0.07	$gN.gCOD_X^{-1}$	(1)
inxi	N fraction of inert biomass	0.018	$gN.gCOD_{Xi}^{-1}$	(3)
K_{FA}	Affinity constant for free ammonia	0.05	$gN.m^{-3}$	(8)
K_{FNA}	Affinity constant for free nitrous acid	5.00E-06	$gN.m^{-3}$	(8)
$K_{I3,NO}$	H NO inhibition coefficient $NO_2^- \rightarrow NO$	0.5	$gN.m^{-3}$	(2)
$K_{I4,NO}$	H NO inhibition coefficient $NO \rightarrow N_2O$	0.3	$gN.m^{-3}$	(2)
$K_{I5,NO}$	H NO inhibition coefficient $N_2O \rightarrow N_2$	0.075	$gN.m^{-3}$	(2)
$K_{I,FA,AOB}$	AOB inhibition coefficient for FA	1	$gN.m^{-3}$	(2)
$K_{I,FA,NOB}$	NOB inhibition coefficient for FA	0.2	$gN.m^{-3}$	(2)
$K_{N2O,H}$	H affinity constant for N_2O	0.05	$gN.m^{-3}$	(2)

$K_{NH,H}$	H affinity constant for NH_4	0.01	$gN.m^{-3}$	(2)
$K_{NO2,H}$	H affinity constant for NO_{2-}	0.2	$gN.m^{-3}$	(2)
$K_{NO3,H}$	H affinity constant for NO_{3-}	0.2	$gN.m^{-3}$	(2)
$K_{NO,H}$	H affinity constant for NO	0.05	$gN.m^{-3}$	(2)
$K_{O,H}$	H affinity constant for O_2 - aerobic growth	0.2	$gO_2.m^{-3}$	(3)
$K_{O,H2}$	H affinity constant for O_2 - anoxic growth $NO_3^- \rightarrow NO_{2-}$	0.2	$gO_2.m^{-3}$	(3)
$K_{O,H3}$	H affinity constant for O_2 - anoxic growth $NO_2^- \rightarrow NO$	0.2	$gO_2.m^{-3}$	(3)
$K_{O,H4}$	H affinity constant for O_2 - anoxic growth $NO \rightarrow N_2O$	0.2	$gO_2.m^{-3}$	(3)
$K_{O,H5}$	H affinity constant for O_2 - anoxic growth $N_2O \rightarrow N_2$	0.2	$gO_2.m^{-3}$	(3)
$K_{O,AOB}$	AOB affinity constant for O_2	0.5	$gO_2.m^{-3}$	(3)
$K_{O,NOB}$	NOB affinity constant for O_2	1	$gO_2.m^{-3}$	(3)
$K_{S,H}$	H affinity constant for Ss - aerobic growth	0.6	$gCOD.m^{-3}$	(3)
$K_{S,H,2}$	H affinity constant for Ss - anoxic growth $NO_3^- \rightarrow NO_{2-}$	0.6	$gCOD.m^{-3}$	(3)
$K_{S,H,3}$	H affinity constant for Ss - anoxic growth $NO_2^- \rightarrow NO$	0.6	$gCOD.m^{-3}$	(3)
$K_{S,H,4}$	H affinity constant for Ss - anoxic growth $NO \rightarrow N_2O$	0.6	$gCOD.m^{-3}$	(3)
$K_{S,H,5}$	H affinity constant for Ss - anoxic growth $N_2O \rightarrow N_2$	0.6	$gCOD.m^{-3}$	(3)
K_{STO}	H affinity constant for X_{STO}	1	$gCOD_{XSTO}.gCOD_{XH}^{-1}$	(3)
k_{STO}	Maximum rate of storage	1.25	d^{-1}	(8)
μ_{AOB}	AOB maximum specific growth rate	0.6	d^{-1}	(8)
$\mu_{H,S}$	H maximum specific growth rate on Ss	2.6	d^{-1}	(3)
$\mu_{H,STO}$	H maximum specific growth rate on X_{STO}	2.6	d^{-1}	(3)
μ_{NOB}	NOB maximum specific growth rate	0.6	d^{-1}	(8)
Y_{AOB}	Autotrophic yield of AOB	0.15	$gCOD_{XAOB}.gN^{-1}$	(7)
$Y_{H,S}$	H yield on Ss - aerobic	0.63	$gCOD_{XH}.gCOD_{SS}^{-1}$	(1)
$Y_{H,STO}$	H yield on X_{STO} - aerobic	0.68	$gCOD_{XH}.gCOD_{XSTO}^{-1}$	(3)
$Y_{H,STO,anox}$	H yield on X_{STO} - anoxic	0.57	$gCOD_{XH}.gCOD_{XSTO}^{-1}$	(3)
$Y_{H,S,anox}$	H yield on Ss - anoxic	0.63	$gCOD_{XH}.gCOD_{SS}$-1	(8)
Y_{NOB}	Autotrophic yield of NOB	0.09	$gCOD_{XNOB}.gN^{-1}$	(7)
Y_{STO}	Storage yield on S_S - aerobic	0.85	$gCOD_{XSTO}.gCOD_{SS}^{-1}$	(3)
$Y_{STO,anox}$	Storage yield on S_S - anoxic	0.81	$gCOD_{XSTO}.gCOD_{SS}^{-1}$	(3)
ro_{N2O}	partial pressure of N_2O	3.00E-07	atm	(4)
ro_{NO}	partial pressure of NO (neglected)	0	atm	-
KH_{N2O}	Henry's law constant for solubility in water at 298.15 K	350	$gN.m^{-3}.atm^{-1}$	(6)
KH_{NO}	Henry's law constant for solubility in water at 298.15 K	26.6	$gN.m^{-3}.atm^{-1}$	(6)